Published OnlineFirst November 14, 2010; DOI:10.1158/1078-0432.CCR-10-1371

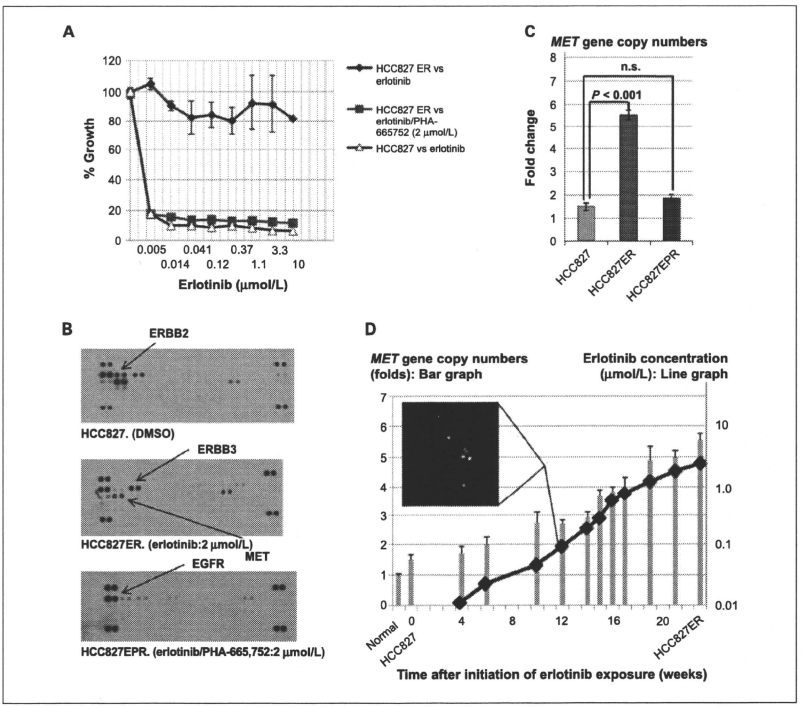

Fig. 1. Amplified *MET* gene caused erlotinib resistance in HCC827ER cells but not in HCC827EPR cells. A, HCC827ER cells were resistant to erlotinib, and PHA-665,752 restored erlotinib sensitivity. HCC827 or HCC827ER cells were incubated for 24 hours and for an additional 72 hours with the indicated concentrations of erlotinib with or without 2 μmol/L PHA-665,752, and cell growth was determined. B, activated RTKs identified by the Human Phospho-RTK Array Kit. Whole-cell extracts from HCC827, HCC827ER, and HCC827EPR exposed for 24 hours to the indicated drug(s) were incubated in the RTK arrays, and the phosphorylation status was determined by subsequent incubation with a horseradish peroxidase–conjugated phosphor-tyrosine detection antibody. Each RTK was spotted in duplicate and the pairs of dots in each corner are the positive controls. C, *MET* gene was amplified in HCC827ER cells but not in HCC827EPR cells. *MET* gene copy numbers were measured by quantitative real-time PCR. Normal genomic DNA was used as a standard sample. D, *MET* gene copy numbers in HCC827ER progenitor cells. Relative *MET* gene copy numbers (columns) were measured by real-time quantitative PCR in HCC827ER and their progenitor cells with incomplete erlotinib resistance. One division on the abscissa indicates 1 week after initiation of erlotinib exposure; left ordinate, the *MET* gene copy number; right ordinate, erlotinib concentration (μmol/L) at the each time. *MET* gene copy number data are presented as the mean ± SD of triplicate experiments. Hybridization of MET/CEP7 probe set with HCC827ER80 cells is also shown.

RTKs and both positive and negative controls. HCC827, HCC827ER, and HCC827EPR cells were cultured in 10-cm plates in RPMI1640 with 5% FBS until subconfluent. The media were changed to 5% FBS containing DMSO, 2 μmol/L erlotinib, and a combination of 2 μmol/L erlotinib/PHA-665,752, respectively, for 24 hours, and the cells were lysed by NP-40 lysis buffer according to the manufacturer's protocol. The arrays were blocked with blocking buffer and incubated with 450 μg of cell lysate overnight at 4°C. The arrays were washed, incubated with a horseradish peroxidase–conjugated phospho-tyrosine detection antibody, treated with ECL solution, and exposed to film.

Preparation of DNA and RNA

Genomic DNA was extracted using a FastPure DNA Kit (Takara Bio) according to the manufacturer's protocol. Total RNA was prepared using a mirVana miRNA Isolation Kit (Qiagen), according to the manufacturer's protocol.

Published OnlineFirst November 14, 2010; DOI:10.1158/1078-0432.CCR-10-1371

Random-primed, first-strand cDNA was synthesized from 10 μg of total RNA using Superscript II (Invitrogen) according to the manufacturer's instructions.

Mutation analysis

Mutation analysis of exons 18 to 21 of the *EGFR* gene, exons 1 to 2 of the *KRAS* gene, and exon 20 of the human epidermal growth factor receptor 2 (*HER2*) gene was done by direct sequencing after one-step reverse transcriptase-PCR (RT-PCR) using the Qiagen OneStep Reverse Transcription-PCR Kit (Qiagen) using total RNA as reported previously (17, 21). In the clinical autopsy samples, the *EGFR* mutation was analyzed using the Cycleave PCR technique and fragment analysis as described previously (22). Use of both methods enabled us to detect three types of G719 point mutations: exon 19 deletion mutations, exon 20 insertion mutations, and T790M, L858R, or L861Q point mutations.

Gene copy number analysis

The copy number of the *MET* gene relative to a *LINE-1* repetitive element was measured by quantitative real-time PCR using the SYBR Green Method (Power SYBR Green PCR Master Mix; Qiagen) with an ABI PRISM 7900HT Sequence Detection System (Applied Biosystems) as described previously (11, 17). PCR was done in triplicate for each primer set. HCC827 incomplete erlotinib-resistant cells were analyzed for genomic status of *MET* by fluorescence *in situ* hybridization (FISH) using a D7S522 probe and chromosome 7 centromere probe (CEP7) purchased from Vysis and following the protocol described previously (11). The copy number of the *EGFR* gene relative to *LINE-1* was analyzed in the same way using primers for *EGFR* exon 21 that was described previously (2). *LINE-1* was used as the internal control because the copy number of *LINE-1* is reported to be similar in normal

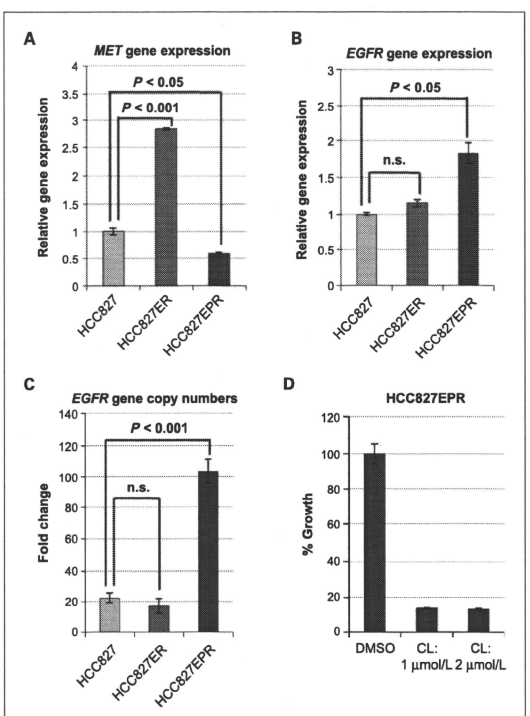

Fig. 2. Increased dependency on EGFR in HCC827EPR cells. A, *MET* gene expression increased in HCC827ER cells but decreased in HCC827EPR cells. B, *EGFR* gene expression increased in HCC827EPR cells. Quantitative real-time RT-PCR was done using validated TaqMan probes. The assays were done in triplicate, and the expression level of 18S rRNA was used as the internal control. n.s., not significant. C, the *EGFR* gene was amplified in HCC827EPR cells but not in HCC827ER cells. *EGFR* gene copy number was determined by quantitative real-time PCR. Normal genomic DNA was used as the standard sample. D, HCC827EPR cells were sensitive to CL-387,785. HCC827EPR cells were incubated for 24 hours and for an additional 72 hours with the indicated concentrations of CL-387,785 or DMSO, and cell growth was measured.

Published OnlineFirst November 14, 2010; DOI:10.1158/1078-0432.CCR-10-1371

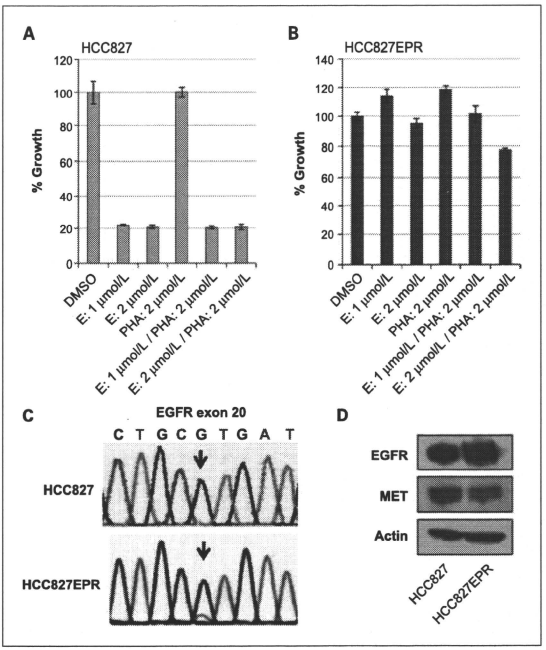

Fig. 3. HCC827EPR cells were resistant to erlotinib and/or PHA-665,752 and harbored the T790M mutation. A, HCC827 cells were sensitive to erlotinib (E) but not to PHA-665,752 (PHA). B, HCC827EPR cells were resistant to erlotinib and to the combination of erlotinib and PHA-665,752. HCC827 and HCC827EPR cells were incubated for 24 hours and for an additional 72 hours with indicated concentrations of drug(s), and cell growth was determined. C, HCC827EPR cells but not HCC827 cells harbored the T790M mutation. Antisense strands of sequencing chromatograms for *EGFR* mRNA are shown. Black arrow, C to T substitution at nucleotide 2,369 (G to A on the antisense strand), which results in the T790M mutation. D, Western blot analysis of EGFR and MET in HCC827 and HCC827EPR cells. Expression of β-actin was used as the control.

and cancerous cells (23). Normal genomic DNA was used as a standard sample.

Quantitative real-time RT-PCR

Quantitative real-time RT-PCR was done using first-strand cDNA with TaqMan probes and TaqMan Universal PCR Master Mix (Applied Biosystems). TaqMan probes for *EGFR* and *MET* were purchased from Applied Biosystems, and the amplification was done using an ABI PRISM 7900HT Sequence Detection System (Applied Biosystems) according to the manufacturer's instructions. Quantification was done in triplicate, and the expression levels of 18S rRNA were used as the internal control. The expression value for each resistant cell line was calculated relative to that of the HCC827 parent cells.

Antibodies and Western blot analysis

Anti-EGFR and anti-MET antibodies were purchased from Cell Signaling Technology. Anti-β-actin antibody was purchased from Sigma. Preparation of total cell lysates and immunoblotting were carried out as described previously (24). Briefly, cells were cultured until subconfluent and lysed in SDS sample buffer and homogenized. Total cell lysate (30 ug) was subjected to SDS-PAGE and transferred to Immobilon-P polyvinylidene difluoride membranes (Millipore). Following blocking with 5% nonfat dry milk, the membranes were incubated with the primary antibody, washed with PBS, reacted with the secondary antibody, treated with ECL solution, and exposed to film.

Clinical autopsy samples

Autopsy samples from six lung adenocarcinoma patients harboring multiple gefitinib-refractory tumors were included. All patients responded to gefitinib monotherapy and experienced disease progression while on continuous treatment with gefitinib. These patients met the recently proposed criteria for acquired resistance to EGFR-TKIs (25). Approval from the institutional review board of Higashihiroshima Medical Center for the use of the tumor tissue specimens was obtained from the legal guardians of the patients. The patients' characteristics

Published OnlineFirst November 14, 2010; DOI:10.1158/1078-0432.CCR-10-1371

Table 2. *EGFR* mutational status and *MET* gene amplification in each primary or metastatic lesion

Patient	Primary	IM	LNs	Liver	Ad-G	Oment	Pleura
1	NA	DEL/T	DEL/T	DEL/m	—	DEL/T/M	—
2	DEL/T/m	—	DEL/M	DEL/T/m	DEL/T/m	—	—
3	DEL/M	DEL/M*	—	DEL/M	DEL/M	DEL/M	—
4	NE	—	—	—	—	—	DEL/T
5	L858R/T	—	—	—	—	—	L858R/T
6	DEL	DEL/T*	DEL/T†	—	—	—	—

(*Continued on the following page*)

are summarized in Table 1. There were three men and three women. Four patients were nonsmokers and two were smokers. One patient had recurrent disease after surgery (patient 1), whereas five patients were nonsurgical cases (patients 2-6). The initial tumor responses to gefitinib were assessed according to the Response Evaluation Criteria in Solid Tumors (26).

Statistical analyses

Statistical analysis was carried out using StatView version 5.01 (SAS Institute). $P < 0.05$ was considered significant. All tests were two-sided.

Results

MET amplification causes resistance to erlotinib in HCC827ER cells

We first generated *in vitro* clones of HCC827 cells that were resistant to erlotinib (designated as HCC827ER) by growing cells in increasing concentrations of erlotinib to a final concentration of 2 μmol/L for up to 6 months, as described previously (11, 14, 27). HCC827ER was >2,000 times as resistant to erlotinib as the parental HCC827. Proliferation declined by <20% in HCC827ER cells incubated at erlotinib concentrations up to 10 μmol/L, whereas only 10% of parental HCC827 cells survived after exposure to 14 nmol/L erlotinib (Fig. 1A). The RTK array of HCC827ER cells showed activation of MET and ERBB3 in the presence of 2 μmol/L erlotinib (Fig. 1B), which was similar to that observed in a previous study (11). The *MET* gene copy number of HCC827ER cells assessed by quantitative real-time PCR was a 5.5-fold gain compared with normal DNA (Fig. 1C). We also used quantitative real-time PCR to confirm that the increased gene dose led to increased *MET* gene expression (Fig. 2A). On the other hand, no secondary mutations, including T790M, in exons 18 to 21 of the *EGFR* gene or a mutation in exons 1 to 2 of the *KRAS* gene were detected in HCC827ER cells. The contribution of *MET* amplification to erlotinib resistance was confirmed by the observation that a MET inhibitor, PHA-665,752, restored erlotinib sensitivity in HCC827ER cells (Fig. 1A).

Clinically relevant erlotinib resistance occurs at a 4-fold *MET* amplification

MET gene copy number was monitored in the developing HCC827ER cells. The *MET* gene copy number increased in proportion to erlotinib resistance (Fig. 1D). To distinguish small gains in *MET* gene copy number across all cells in the pool from an increase in the percentage of highly *MET*-amplified cells in the population, we did FISH of HCC827ER80 cells (HCC827 cells that acquired resistance to 80 nmol/L concentration of erlotinib) and identified that most of the cells harbored moderate *MET* gene copy number gains. When *MET* gene copy number had increased by >4-fold, the cells were able to proliferate in the presence of micromolar concentrations of a TKI, which is achievable clinically (e.g., the maximum drug concentration for a dose of 300 mg gefitinib and of 150 mg erlotinib was 0.85 μmol/L and 4.0 μmol/L, respectively; refs. 28, 29).

Generation of HCC827EPR cells

We then asked what would happen when we treated HCC827 cells with increasing concentrations of erlotinib in the presence of a MET inhibitor. We generated erlotinib-resistant HCC827 cells in the same way up to a final concentration of 2 μmol/L in the presence of 1 μmol/L PHA-665,752 for up to 9 months. We first confirmed the identity of the resultant resistant HCC827 cells to erlotinib plus PHA-665,752 (designated as HCC827EPR) by analyzing 10 loci of STR profiling and comparing them with the 9 loci of STR data of HCC827 provided by the American Type Culture Collection. The evaluation values of each pair of cell lines, HCC827 versus HCC827ER, HCC827 versus HCC827EPR, and HCC827ER versus HCC827EPR, were all 1.0, indicating complete identity of all analyzed STR loci.

HCC827 parental cells were resistant to the treatment with PHA-665,752 alone (Fig. 3A). The HCC827EPR cells were also resistant to 2 μmol/L erlotinib plus 2 μmol/L PHA-665,752 and could be maintained in medium with 2 μmol/L of both drugs. In contrast to the parental HCC827 cells, HCC827EPR cells were resistant to erlotinib alone, PHA-665,752 alone, and the combination of both drugs in the growth-inhibition assay (Fig. 3A and B). The RTK array did not detect activated RTKs except for EGFR

Published OnlineFirst November 14, 2010; DOI:10.1158/1078-0432.CCR-10-1371

Table 2. *EGFR* mutational status and *MET* gene amplification in each primary or metastatic lesion (Cont'd)

Kidney	Chest	Ret-P	Skin	Thyroid	Bowel	Heart	Bone
	—	DEL/T	DEL/M	—	—	—	—
DEL/T/m	—	—	—	DEL/T	—	—	—
DEL/M	DEL/M	—	—	—	DEL/M	DEL/M	—
—	—	—	—	—	—	—	DEL/T
—	L858R/T	—	—	—	—	—	—
—	—	—	—	—	—	—	—

Abbreviations: IM, intrapulmonary metastasis; LN, mediastinal or hilar lymph nodes; Ad-G, adrenal gland; Oment, omentum; Chest, chest wall; Ret-P, retroperitoneum; Bowel, small intestine; NA, not available; DEL, exon 19 deletion mutation; T, T790M mutation; m, *MET* gene copy number gain (2- to 4-fold compared with normal); M, *MET* gene amplification (≥4-fold); NE, not evaluable because of lack of viable tumor cells.

*Two independent intrapulmonary metastatic lesions were analyzed and both harbored the same genetic alterations.

†Three independent lymph nodes, 10R, 7, and 4L, were analyzed and all harbored the same genetic alterations.

under the inhibition of 2 μmol/L erlotinib and 2 μmol/L PHA-665,752 (Fig. 1B). In addition, the *MET* gene copy number did not increase in HCC827EPR cells (Fig. 1C).

T790M mutation and increased *EGFR* gene copy number developed in HCC827EPR cells

We next sequenced exons 18 to 21 of the *EGFR* gene of HCC827EPR cells and identified the T790M mutation in addition to a homozygous 15 bp deletion in exon 19 (Fig. 3C). The existence of the T790M mutation in HCC827EPR cells but not in HCC827 parental cells was also confirmed by the Cycleave PCR technique (ref. 22; data not shown). The T790M mutation was detected in all three subclones obtained by single cell cloning of HCC827EPR cells. No secondary mutation in exons 1 to 2 of the *KRAS* gene or exon 20 of the *HER2* gene was detected (data not shown). Gene expression analysis revealed significantly increased *EGFR* gene expression (Fig. 2B) and decreased *MET* gene expression (Fig. 2A) in HCC827EPR cells compared with HCC827 cells, and these were consistent with Western blot analysis (Fig. 3D). We next analyzed *EGFR* gene copy number in HCC827 cells and in the resistant cells. HCC827 cells originally harbored 20 times the gene copy number compared with normal DNA (Fig. 2C), confirming the results of a previous study (30). HCC827EPR cells showed a further 5-fold *EGFR* gene amplification (>100-fold gene copy number) compared with the parental HCC827 cells, whereas the gene copy number was similar in HCC827ER cells and HCC827 cells (Fig. 2C). Addition of the irreversible EGFR-TKI CL-387,785 inhibited growth of HCC827EPR cells (Fig. 2D), showing that HCC827EPR cells were still dependent on signaling from the EGFR pathway.

Analysis of multiple gefitinib-refractory tumors obtained from autopsy

Thirty-four gefitinib-refractory lesions produced after an initial good response to gefitinib were available from the six patients. One sample contained almost no viable tumor cells and the resultant 33 lesions were evaluated by molecular analysis (Table 2). *MET* amplification was defined as a copy number gain (CNG) of the *MET* gene of ≥4-fold, on the basis of the *in vitro* data (described above) and previous studies (11, 14). A CNG of the *MET* gene of <4-fold was defined as a moderate *MET* gene CNG.

Each patient harbored the identical activating mutations of the *EGFR* gene in their tumors (five patients with an exon 19 deletion and one with L858R; Table 2). As the mechanism of acquired resistance, 31 of 33 lesions had T790M and/or *MET* amplification. Nine lesions from patient 3 all had *MET* amplification without T790M. By contrast, all two lesions from patient 4, all three lesions from patient 5, and five of six lesions from patient 6 had T790M without *MET* amplification. Interestingly, the lesions from patients 1 and 2 exhibited T790M and/or *MET* amplification depending on the lesion sites. Ten of the 12 gefitinib-refractory lesions from patients 1 and 2 exhibited one of the two resistance mechanisms. The liver tumor from patient 1 had only a minor degree of *MET* CNG (3.2-fold), whereas the metastatic lesion from the omentum of patient 1 harbored both resistant mechanisms. Moderate *MET* CNGs were found in five lesions obtained only from these two patients (designated "m" in Table 2) but not in other patients, suggesting that the tumors in these two patients had the ability to develop *MET* amplification. We compared the relationship between the presence of T790M and *MET* gene copy number. The T790M mutation developed in 93% (14 of 15) of tumors without *MET* gene CNGs, in 80% (4 of 5) of tumors with moderate *MET* gene CNGs, and in only 8% (1 of 13) of tumors with *MET* amplification (Fig. 4A). This finding suggests that there was a reciprocal and complementary relationship between *MET* amplification and the T790M mutation.

Discussion

We found that HCC827 became resistant to erlotinib because of *MET* amplification, which is similar to the

Published OnlineFirst November 14, 2010; DOI:10.1158/1078-0432.CCR-10-1371

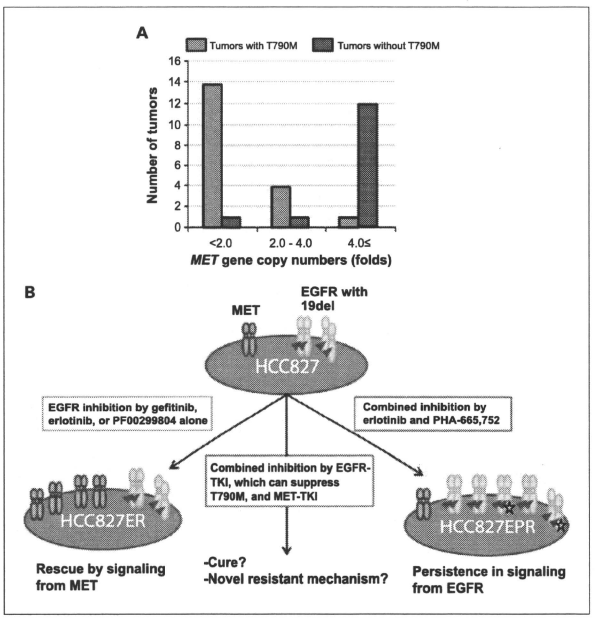

Fig. 4. Reciprocal relationship between *MET* amplification and T790M mutation. A, tumor numbers with or without T790M mutation by *MET* gene copy numbers in gefitinib-refractory tumors obtained from autopsy. B, schema of the difference of escape hatches of HCC827 cells depending on the selection pressure differences by molecular target drug(s). All amplified EGFR alleles harbor exon 19 deletion mutation in HCC827 cells, and a part of them in HCC827EPR cells acquired T790M mutation (yellow stars).

acquired resistance to gefitinib (11) or to an irreversible pan-ERBB kinase inhibitor, PF00299804 (14). We also found that the *MET* CNG increased in proportion to erlotinib resistance and that a ≥4-fold *MET* CNG compared with normal DNA was an apparent threshold for the development of clinically relevant TKI resistance. This observation is consistent with the observation that a moderate *MET* CNG (<4-fold) could coexist with T790M but that *MET* gene amplification (≥4-fold) and T790M were almost mutually exclusive in our autopsy analysis.

On the other hand, PC9 (exon 19 deletion) and H3255 (L858R) are known to develop resistance to EGFR-TKIs through T790M (18–20, 31). These phenomena are explained by the existence of minor clones with such alterations before EGFR-TKI treatment. Supporting this hypothesis further, Turke et al. found 0.06% to 0.14% of *MET*-amplified minor subclones in HCC827 but not in PC9 or H3255 cells (14). In addition, Inukai and Maheswaran showed that patients with *EGFR* mutations had shorter progression-free survival when the tumor had a very small amount of T790M before the EGFR-TKI therapy (13, 32). Thus, it seems that these cell lines are destined to use either mechanism to overcome EGFR-TKIs. It is interesting that HCC827 cells developed the T790M mutation when exposed to increasing concentrations of erlotinib under the inhibition of MET signaling (Fig. 4B), although it took about 1.5 times longer compared with erlotinib alone. The origin of the T790M allele in HCC827 cells is not clear, although this is the case with other *in vitro* gefitinib-resistant models used to develop the T790M mutation (PC9 and H3255 cell lines; refs. 18, 31). More sensitive methods might be able to detect the presence of minor clones with the T790M mutation in these cell lines before the start of EGFR-TKI treatment.

No studies have investigated the mechanisms responsible for the acquired resistance to EGFR-TKI therapy in multiple sites of metastases obtained from autopsy. The autopsy samples allowed us to see the ultimate pictures of resistance and to examine multiple organ sites simultaneously. Thirty-one of 33 lesions harbored the T790M mutation and/or *MET* amplification. We also found an inverse relationship between the presence of T790M and *MET* gene copy number, suggesting a complementary role of the two mechanisms in the acquisition of resistance. This is consistent with a previous report; one of the patients with acquired resistance to EGFR-TKI harbored

Published OnlineFirst November 14, 2010; DOI:10.1158/1078-0432.CCR-10-1371

two tumors, one with *MET* amplification only and the other with moderate *MET* CNG and T790M (12). The incidence of the T790M mutation and *MET* amplification as mechanisms responsible for the acquired resistance to EGFR-TKIs was reported to be ~50% and ~20%, respectively (33). However, our present results suggest that the incidence of these two mechanisms is higher in the later phase and that overcoming these two mechanisms would be the key to improving patient outcomes further.

The factors that determine which mechanism will be used by tumor cells for overcoming EGFR-TKIs are not clear. One may speculate that the balance between positive and negative regulators of the MET pathway in the microenvironment of the tumor cells determines the mechanisms of resistance. Hepatocyte growth factor, a ligand for MET, has been shown recently to induce transient and reversible resistance to EGFR-TKIs (34, 35) and to facilitate *in vitro MET* amplification in the development of stable acquired resistance to EGFR-TKIs (14). On the other hand, there are several negative regulators of the HGF-MET axis. One example is to increase MET degradation by Cbl-mediated ubiquitination or another mechanism. Overexpression of LRIG1, a transmembrane leucine-rich repeat and immunoglobulin-like domain-containing protein, destabilizes MET and impairs the ability to respond to hepatocyte growth factor (36). Another possibility is a negative regulator of MET-induced cell behavior, such as Abl tyrosine kinase, which functions as a negative regulator of MET-induced cell motility via phosphorylation of the adapter protein CrkII (37).

In conclusion, we observed a reciprocal, complementary relationship between *MET* amplification and the *EGFR* T790M mutation in both an *in vitro* erlotinib-resistant model (illustrated in Fig. 4B) and in our analysis of gefitinib-refractory tumors obtained from autopsy samples. Molecular target therapy prolongs the overall survival in lung cancer patients with an *EGFR* mutation (38), and the development of the concurrent inhibition therapy might be essential for the further improvement.

Disclosure of Potential Conflicts of Interest

T. Mitsudomi has received lecture fees from AstraZeneca and Chugai. The other authors declare no conflict of interest.

Acknowledgments

We thank Ms. Noriko Shibata for excellent technical assistance in the molecular analysis, Dr. Adi F. Gazdar for providing cell lines, and Hoffmann-La Roche, Inc. for kindly providing erlotinib.

Grant Support

Financial support for this study was provided by a Grant-in-Aid for Scientific Research (B) from the Japan Society for the Promotion of Science (20903076) and by a grant from the Kobayashi Institute for Innovative Cancer Chemotherapy.

The costs of publication of this article were defrayed in part by the payment of page charges. This article must therefore be hereby marked *advertisement* in accordance with 18 U.S.C. Section 1734 solely to indicate this fact.

Received 05/20/2010; revised 08/06/2010; accepted 08/21/2010; published OnlineFirst 11/09/2010.

References

1. Lynch TJ, Bell DW, Sordella R, et al. Activating mutations in the epidermal growth factor receptor underlying responsiveness of non-small-cell lung cancer to gefitinib. N Engl J Med 2004;350:2129–39.
2. Paez JG, Janne PA, Lee JC, et al. EGFR mutations in lung cancer: correlation with clinical response to gefitinib therapy. Science 2004; 304:1497–500.
3. Mitsudomi T, Yatabe Y. Mutations of the epidermal growth factor receptor gene and related genes as determinants of epidermal growth factor receptor tyrosine kinase inhibitors sensitivity in lung cancer. Cancer Sci 2007;98:1817–24.
4. Mok TS, Wu YL, Thongprasert S, et al. Gefitinib or carboplatin-paclitaxel in pulmonary adenocarcinoma. N Engl J Med 2009;361: 947–57.
5. Mitsudomi T, Morita S, Yatabe Y, et al. Gefitinib versus cisplatin plus docetaxel in patients with non-small-cell lung cancer harbouring mutations of the epidermal growth factor receptor (WJTOG3405): an open label, randomised phase 3 trial. Lancet Oncol 2010;11:121–8.
6. Pao W, Miller V, Zakowski M, et al. EGF receptor gene mutations are common in lung cancers from "never smokers" and are associated with sensitivity of tumors to gefitinib and erlotinib. Proc Natl Acad Sci U S A 2004;101:13306–11.
7. Rosell R, Moran T, Queralt C, et al. Screening for epidermal growth factor receptor mutations in lung cancer. N Engl J Med 2009;361: 958–67.
8. Morita S, Hirashima T, Hagiwara K, et al. Gefitinib combined survival analysis of the mutation positives from the prospective phase II trials (I-CAMP). J Clin Oncol 2008;26:abst 8101.
9. Kobayashi S, Boggon TJ, Dayaram T, et al. EGFR mutation and resistance of non-small-cell lung cancer to gefitinib. N Engl J Med 2005;352:786–92.
10. Pao W, Miller VA, Politi KA, et al. Acquired resistance of lung adenocarcinomas to gefitinib or erlotinib is associated with a second mutation in the EGFR kinase domain. PLoS Med 2005;2:e73.
11. Engelman JA, Zejnullahu K, Mitsudomi T, et al. MET amplification leads to gefitinib resistance in lung cancer by activating ERBB3 signaling. Science 2007;316:1039–43.
12. Bean J, Brennan C, Shih JY, et al. MET amplification occurs with or without T790M mutations in EGFR mutant lung tumors with acquired resistance to gefitinib or erlotinib. Proc Natl Acad Sci U S A 2007; 104:20932–7.
13. Inukai M, Toyooka S, Ito S, et al. Presence of epidermal growth factor receptor gene T790M mutation as a minor clone in non-small cell lung cancer. Cancer Res 2006;66:7854–8.
14. Turke AB, Zejnullahu K, Wu YL, et al. Preexistence and clonal selection of MET amplification in EGFR mutant NSCLC. Cancer Cell 2010; 17:77–88.
15. Toyooka S, Kiura K, Mitsudomi T. EGFR mutation and response of lung cancer to gefitinib. N Engl J Med 2005;352:2136, author reply.
16. Kubo T, Yamamoto H, Lockwood WW, et al. MET gene amplification or EGFR mutation activate MET in lung cancers untreated with EGFR tyrosine kinase inhibitors. Int J Cancer 2009;124:1778–84.
17. Onozato R, Kosaka T, Kuwano H, Sekido Y, Yatabe Y, Mitsudomi T. Activation of MET by gene amplification or by splice mutations deleting the juxtamembrane domain in primary resected lung cancers. J Thorac Oncol 2009;4:5–11.
18. Ogino A, Kitao H, Hirano S, et al. Emergence of epidermal growth factor receptor T790M mutation during chronic exposure to gefitinib in a non small cell lung cancer cell line. Cancer Res 2007;67:7807–14.
19. Yoshida T, Okamoto I, Okamoto W, et al. Effects of Src inhibitors on cell growth and epidermal growth factor receptor and MET signaling

Published OnlineFirst November 14, 2010; DOI:10.1158/1078-0432.CCR-10-1371

in gefitinib-resistant non-small cell lung cancer cells with acquired MET amplification. Cancer Sci 2010;101:167–72.
20. Ercan D, Zejnullahu K, Yonesaka K, et al. Amplification of EGFR T790M causes resistance to an irreversible EGFR inhibitor. Oncogene 2010;29:2346–56.
21. Kosaka T, Yatabe Y, Endoh H, et al. Analysis of epidermal growth factor receptor gene mutation in patients with non-small cell lung cancer and acquired resistance to gefitinib. Clin Cancer Res 2006; 12:5764–9.
22. Yatabe Y, Hida T, Horio Y, Kosaka T, Takahashi T, Mitsudomi T. A rapid, sensitive assay to detect EGFR mutation in small biopsy specimens from lung cancer. J Mol Diagn 2006;8:335–41.
23. Zhao X, Weir BA, LaFramboise T, et al. Homozygous deletions and chromosome amplifications in human lung carcinomas revealed by single nucleotide polymorphism array analysis. Cancer Res 2005;65: 5561–70.
24. Usami N, Fukui T, Kondo M, et al. Establishment and characterization of four malignant pleural mesothelioma cell lines from Japanese patients. Cancer Sci 2006;97:387–94.
25. Jackman D, Pao W, Riely GJ, et al. Clinical definition of acquired resistance to epidermal growth factor receptor tyrosine kinase inhibitors in non-small-cell lung cancer. J Clin Oncol 2010;28:357–60.
26. Therasse P, Arbuck SG, Eisenhauer EA, et al. New guidelines to evaluate the response to treatment in solid tumors. European Organization for Research and Treatment of Cancer, National Cancer Institute of the United States, National Cancer Institute of Canada. J Natl Cancer Inst 2000;92:205–16.
27. Martha Guix, Anthony C. Faber, Shizhen Emily Wang, et al. Acquired resistence to EGFR tyrosine kinase inhibitors in cancer cells is mediated by loss of IGF-binding proteins. J Clin Invest 2008;118: 2609–19.
28. Ranson M, Turke JAE, Ferry D, et al. ZD1839, a selective oral epidermal growth factor receptor-tyrosine kinase inhibitor, is well tolerated and active in patients with solid, malignant tumors: results of a phase I trial. J Clin Oncol 2002;20:2240–50.
29. Hidalgo M, Siu LL, Nemunaitis J, et al. Phase I and pharmacologic study of OSI-774, an epidermal growth factor receptor tyrosine kinase inhibitor, in patients with advanced solid malignancies. J Clin Oncol 2001;19:3267–79.
30. Gandhi J, Zhang J, Xie Y, et al. Alterations in genes of the EGFR signaling pathway and their relationship to EGFR tyrosine kinase inhibitor sensitivity in lung cancer cell lines. PloS One 2009;4:e4576.
31. Engelman JA, Mukohara T, Zejnullahu K, et al. Allelic dilution obscures detection of a biologically significant resistance mutation in EGFR-amplified lung cancer. J Clin Invest 2006;116:2695–706.
32. Maheswaran S, Sequist LV, Nagrath S, et al. Detection of mutations in EGFR in circulating lung-cancer cells. N Engl J Med 2008;359:366–77.
33. Suda K, Onozato R, Yatabe Y, Mitsudomi T. EGFR T790M mutation: a double role in lung cancer cell survival? J Thorac Oncol 2009;4:1–4.
34. Yano S, Wang W, Li Q, et al. Hepatocyte growth factor induces gefitinib resistance of lung adenocarcinoma with epidermal growth factor receptor-activating mutations. Cancer Res 2008;68:9479–87.
35. Yamada T, Matsumoto K, Wang W, et al. Hepatocyte growth factor reduces susceptibility to an irreversible epidermal growth factor receptor inhibitor in EGFR-T790M mutant lung cancer. Clin Cancer Res 2010;16:174–83.
36. Shattuck DL, Miller JK, Laederich M, et al. LRIG1 is a novel negative regulator of the Met receptor and opposes Met and Her2 synergy. Mol Cell Biol 2007;27:1934–46.
37. Cipres A, Abassi YA, Vuori K. Abl functions as a negative regulator of Met-induced cell motility via phosphorylation of the adapter protein CrkII. Cell Signal 2007;19:1662–70.
38. Takano T, Fukui T, Ohe Y, et al. EGFR mutations predict survival benefit from gefitinib in patients with advanced lung adenocarcinoma: a historical comparison of patients treated before and after gefitinib approval in Japan. J Clin Oncol 2008;26:5589–95.

UICC
global cancer control

IJC
International Journal of Cancer

Characteristic methylation profile in CpG island methylator phenotype-negative distal colorectal cancers

Byonggu An[1,2], Yutaka Kondo[1], Yasuyuki Okamoto[1], Keiko Shinjo[1,3], Yukihide Kanemitsu[4], Koji Komori[4], Takashi Hirai[4], Akira Sawaki[5], Masahiro Tajika[5], Tsuneya Nakamura[5], Kenji Yamao[5], Yasushi Yatabe[6], Makiko Fujii[1], Hideki Murakami[1], Hirotaka Osada[1,3], Tohru Tani[7], Keitaro Matsuo[7], Lanlan Shen[8], Jean-Pierre J. Issa[8] and Yoshitaka Sekido[1,3]

[1] Division of Molecular Oncology, Aichi Cancer Center Research Institute, Chikusa-Ku, Nagoya 464-8681, Japan
[2] Department of Surgery, Shiga University of Medical Science, Seta Tsukinowa-cho, Otsu City, Shiga 520-2192, Japan
[3] Department of Cancer Genetics, Program in Function Construction Medicine, Nagoya University Graduate School of Medicine, Showa-ku, Nagoya, 466-8550, Japan
[4] Department of Gastroenterological Surgery, Aichi Cancer Center Central Hospital, Chikusa-Ku, Nagoya 464-8681, Japan
[5] Department of Gastroenterology, Aichi Cancer Center Central Hospital, Chikusa-Ku, Nagoya 464-8681, Japan
[6] Department of Pathology and Molecular Diagnostics, Aichi Cancer Center Hospital, Chikusa-Ku, Nagoya 464-8681, Japan
[7] Division of Epidemiology and Prevention, Aichi Cancer Center Research Institute, Chikusa-Ku, Nagoya 464-8681, Japan
[8] Department of Leukemia, The University of Texas at M.D. Anderson Cancer Center, Houston, TX 77030, USA

Aberrant DNA methylation is involved in colon carcinogenesis. Although the CpG island methylator phenotype (CIMP) is defined as a subset of colorectal cancers (CRCs) with remarkably high levels of DNA methylation, it is not known whether epigenetic processes are also involved in CIMP-negative tumors. We analyzed the DNA methylation profiles of 94 CRCs and their corresponding normal-appearing colonic mucosa with 11 different markers, including the five classical CIMP markers. The CIMP markers were frequently methylated in proximal CRCs ($p < 0.01$); however, *RASSF1A* methylation levels were significantly higher in distal CRCs, the majority of which are CIMP-negative ($p < 0.05$). Similarly, methylation levels of *RASSF1A* and *SFRP1* in the normal-appearing mucosae of distal CRC cases were significantly higher than those in the proximal CRC cases ($p < 0.05$). They were also positively correlated with age (*RASSF1A*, $p < 0.01$; *SFRP1*, $p < 0.01$). Microarray-based genome-wide DNA methylation analysis of 18 CRCs revealed that 168 genes and 720 genes were preferentially methylated in CIMP-negative distal CRCs and CIMP-positive CRCs, respectively. Interestingly, more than half of the hypermethylated genes in CIMP-negative distal CRCs were also methylated in the normal-appearing mucosae, indicating that hypermethylation in CIMP-negative distal CRCs is more closely associated with age-related methylation. By contrast, more than 60% of the hypermethylated genes in CIMP-positive proximal CRCs were cancer specific ($p < 0.01$). These data altogether suggest that CpG island promoters appear to be methylated in different ways depending on location, a finding which may imply the presence of different mechanisms for the acquisition of epigenetic changes during colon tumorigenesis.

Colorectal cancer (CRC) is one of the most common human malignancies worldwide. CRC cells accumulate several genetic and epigenetic alterations in cancer-related genes to achieve malignant status.[1] Mutations in genes controlling the *KRAS/BRAF*, *APC/β-catenin* and *TP53* pathways are well known for their contribution to tumorigenesis.[2] Epigenetic alterations, including DNA hypermethylation of CpG island promoters and global DNA hypomethylation, have been reported to occur early in colorectal carcinogenesis.[3] Hypermethylation of CpG island promoters is closely associated with the transcriptional silencing of tumor suppressor genes, whereas global hypomethylation can lead to chromosomal instability.[4]

Recent cumulative studies in CRCs have suggested the existence of an accumulation of high rates of aberrant promoter hypermethylation in a subset of CRCs known as the CpG island methylator phenotype (CIMP).[5,6] CIMP-positive CRCs exhibit distinct genetic and clinical features, including high rates of *BRAF* and *KRAS* mutations, low rates of *TP53* mutations, a specific histology (mucinous, poorly differentiated), proximal location and characteristic clinical outcomes.[7] Given these clinicopathological features, CIMP-related carcinogenesis may proceed through a specific pathway in which the

Key words: colon cancer, DNA methylation, microarray, field defect
Additional Supporting Information may be found in the online version of this article.
Grant sponsors: Ministry of Health, Labour and Welfare of Japan Grant-in-Aid for Cancer Research (19-17), Japan Society for the Promotion of Science Grant-in-Aid for Scientific Research, and the Mitsui Life Social Welfare Foundation
DOI: 10.1002/ijc.25225
History: Received 27 Jul 2009; Accepted 19 Jan 2010; Online 3 Feb 2010
Correspondence to: Yutaka Kondo, Division of Molecular Oncology, Aichi Cancer Center Research Institute, 1-1 Kanokoden, Chikusa-ku, Nagoya 464-8681, Japan, Tel.: +81-52-764-2993, Fax: +81-52-764-2993, E-mail: ykondo@aichi-cc.jp

epigenetic changes that occur in premalignant cells determine subsequent genetic changes, thereby fostering the progression of these clones.[8] However, it is not known whether epigenetic processes are also involved in CIMP-negative CRCs that frequently emerge in the distal colon.

It has been suggested that proximal and distal CRCs show differences in epidemiological incidence, morphology and molecular biological characteristics.[9–12] Indeed, CIMP-positive CRCs are more frequently found in the proximal than the distal colon, suggesting that intensive accumulation of aberrant DNA methylation is more closely associated with proximal colon carcinogenesis. In contrast, the significance of aberrant DNA methylation is not well understood in distal colon carcinogenesis, where CIMP-negative CRCs are more common. If distinct mechanisms of colon carcinogenesis exist based on their site of origin, it is possible that the DNA methylation behavior and set of hypermethylated genes in distal CRCs are different from those in proximal CIMP-positive CRCs.

In this study, we analyzed the methylation status of CRCs both quantitatively and genome wide, in addition to other clinical and molecular characteristics. We elicited the significance of DNA methylation in CIMP-negative distal CRC compared with CIMP-positive proximal CRC. We also assessed the methylation status of normal-appearing mucosae by location, since DNA methylation, a factor of the field defect (also known as field cancerization) related to epimutagen exposure that leads to cancer formation, may differ by location and CIMP status.[13]

Material and Methods

Tissue samples

Samples of primary CRCs and their corresponding normal-appearing colonic mucosae were collected in accordance with institutional policy from 95 individuals who underwent surgical resection at the Aichi Cancer Center Central Hospital, Nagoya, Japan. All patients provided written informed consent. The specimens examined showed a high cellularity of cancer cells without definite evidence of necrosis. The corresponding normal-appearing colonic mucosae of CRC patients were sampled from two distinct sites: 2 cm and 10 cm from the cancer. We also obtained colonic biopsy samples of normal-appearing mucosae from the cecum and/or rectum of 38 colon polyp patients and the corresponding colon polyps from 22 patients. Pathological finding of all colon polyps is compatible with adenoma. The proximal colon consists of the cecum, and the ascending and transverse colon, and the distal colon consists of the descending and sigmoid colon, and rectum. Genomic DNA was extracted using a standard phenol-chloroform method.

Bisulfite pyrosequencing methylation analysis and bisulfite sequencing analysis

We performed a bisulfite treatment as previously reported.[14] Briefly, 2 μg of genomic DNA was converted and resuspended in 30 μl of water. DNA methylation levels were measured by a highly quantitative method using pyrosequencing technology with 11 methylation markers (Pyrosequencing AB, Uppsala, Sweden). Each assay included positive controls (samples after SssI treatment; New England Biolabs, Ipswich, MA) and negative controls (samples after whole genomic amplification using GenomiPhi V2; GE Healthcare, Piscataway, NJ), mixing experiments to rule out bias and repeat experiments to assess reproducibility. A detailed protocol of pyrosequencing was described previously.[15,16] The methylation levels at different C sites measured by pyrosequencing were averaged to represent the degree of methylation in each sample for each gene. Bisulfite-PCR products of the *MGMT* and *RASSF1A* promoters and *SFRP1* promoters were cloned and sequenced (Invitrogen, Carlsbad, CA). At least 10 clones were sequenced for each sample. The PCR conditions, primer sequences and sequencing primer sequences of the 11 markers are listed in Supporting Information Table 1.

Methylated CpG island amplification microarray

We analyzed 18 CRCs with methylated CpG island amplification microarray (MCAM; average patient age was 65.5 years, ranging from 44 to 79 years): 7 CIMP-positive proximal CRCs and 11 CIMP-negative distal CRCs. All were randomly selected from CRCs as classified *via* the five CIMP markers. Eight corresponding normal-appearing colonic mucosae from CRC patients (average age was 62.5 years, ranging from 52 to 75 years) were also analyzed with MCAM. Seventeen of the 18 CRCs were derived from the 94 CRC samples examined by pyrosequencing analysis, while one was newly added. As normal controls, we used normal-appearing colonic mucosae from two males and two females who, according to our pyrosequencing analysis, showed no aberrant methylation in any of the 11 markers. The background of the analyzed samples is listed in Supporting Information Table 2. A detailed protocol of MCAM was described previously.[16–18] We used a human custom-promoter array from Agilent Technologies (G4497A; Agilent Technologies, Santa Clara, CA) containing 15,134 probes corresponding to 6,157 unique genes, which we had initially validated by the MCAM method in a previous study.[16] Arrays were scanned on an Agilent scanner and analyzed using Feature Extraction software. Normalization was achieved with a linear per-array algorithm according to the manufacturer's protocol (Agilent Technologies).

Hierarchical clustering analysis

Cluster analysis was performed using an agglomerative hierarchical clustering algorithm (http://rana.lbl.gov/EisenSoftware.htm).[19] For specimen clustering, pairwise similarity measures among specimens were calculated using Cluster 3.0 software or Minitab 15 statistical software (http://www.minitab.com) based on DNA methylation intensity measurements across all genes. Dendrograms and heat maps were

Table 1. Clinicopathologic features of CRC patients by CIMP marker status of the cancerous tissue

Characteristic	Total (n = 94)	CIMP positive, n = 26 (27.7)	CIMP negative, n = 68 (72.3)	*p*
Age (yr)				
Mean	65.2	65.8	64.9	0.66
Range	35–86	45–79	35–86	
Gender				
Female	49 (52.1)	14 (28.6)	35 (71.4)	1.00
Male	45 (47.9)	12 (26.7)	33 (73.3)	
Location[1]				
Proximal	40 (42.6)	17 (42.5)	23 (57.5)	<0.01
Distal	54 (57.4)	9 (16.7)	45 (83.3)	
Stage				
I or II	40 (42.6)	9 (22.5)	31 (77.5)	0.36
III or IV	54 (57.4)	17 (31.5)	37 (68.5)	
Tumor differentiation				
Well/Moderate	86 (91.5)	21 (24.4)	65 (75.6)	0.03
Por	8 (8.5)	5 (62.5)	3 (37.5)	
KRAS mutation				
+	32 (34.0)	9 (28.1)	23 (71.9)	1.00
−	62 (66.0)	17 (27.4)	45 (72.6)	
BRAF mutation				
+	6 (6.4)	5 (83.3)	1 (16.7)	<0.01
−	88 (93.6)	21 (23.9)	67 (76.1)	

Values in parentheses indicate percentages.
[1]Proximal—cecum, ascending and transverse colon; Distal—descending and sigmoid colon and rectum.

constructed using Minitab and TreeView software, respectively. To avoid an artificial effect of excess signal values, signal ratios of greater than 10 were defined as 10 for the clustering analysis.

KRAS, *BRAF* and *p53* genes mutation

Mutations in the *KRAS* gene (codons 12 and 13) and *BRAF* gene (codon 600) were determined by the pyrosequencing method as previously reported.[20,21] Mutations in the *p53* gene (exons 5–8) were determined by direct sequencing analysis.[16] The PCR primer sequences and sequencing primer sequences used are listed in Supporting Information Table 1.

Statistical analysis

All statistical analyses were conducted using StatView for Windows (version 5.0). Associations between methylation status and clinicopathological features were analyzed by an unpaired *t* test (Student *t* test or Welch *t* test) and Fisher's exact test. All reported *p* values were two-sided, with $p < 0.05$ being considered statistically significant. Pearson and Spearman tests were used to determine correlations, with significance set at $p < 0.05$; *r* represents the measure of the relationship between two variables and varies from −1 to +1. Disease-free survival curves were generated with the Kaplan-Meier method. The log-rank test was used to estimate disease-free survival. Disease-free survival was calculated starting from the date of surgical procedure to the date of finding new metastatic lesion or local recurrences from primary CRC.

Results

Relationship between CIMP status and clinicopathological features in CRCs

The DNA methylation status of 94 CRCs was examined by pyrosequencing analysis. Methylation status was analyzed as both continuous variable (methylation level) and categorical variable. Genes with methylation levels greater than 15% were considered methylation-positive, since lower values could not be easily distinguished from background.[6,13,22] Samples with simultaneous methylation of at least two of the five classical CIMP markers (*hMLH1*, *MINT1*, *MINT2*, *MINT31* and *p16*) were considered CIMP-positive.[3] Using this criterion, 26 (27.7%) CRCs were classified as CIMP-positive (Table 1). On comparing the clinicopathological features of the CIMP-positive and CIMP-negative groups, we found that the CIMP-positive group was significantly associated

with proximal location, poor differentiation and *BRAF* mutation ($p < 0.01$, $p = 0.03$ and $p < 0.01$, respectively).

Quantitative methylation analysis in the proximal and distal colon

The majority of CIMP-negative CRCs appears to be located in the distal colon. To assess whether DNA methylation of genes other than the CIMP markers is affected by location, we first quantitatively examined methylation levels in the 94 corresponding normal-appearing colonic mucosae and compared the levels in the proximal and distal colon (Fig. 1*a*). To avoid sampling bias, normal-appearing mucosae of CRC patients were sampled from two distinct regions, 2 cm and 10 cm from the cancer. Because methylation levels of the two regions were highly consistent (Supporting Information Table 3), we will hereafter use the average methylation data. Methylation levels of *RASSF1A* and *SFRP1* were significantly higher in the distal than the proximal normal-appearing mucosae ($p < 0.01$ and $p < 0.05$, respectively). Methylation levels of *RUNX3* and *SFRP5* were 15% at most and showed no difference regardless of location. The classical CIMP markers exhibited very low levels of methylation. These methylation patterns were identical in the normal-appearing mucosae from the 38 colon polyp patients (Fig. 1*a*), suggesting that the accumulation of DNA methylation in certain genes is an early event known to be a field defect that occurs during tumorigenesis.[13]

In cancerous tissues, substantially increased methylation was detected in all of the genes examined (Fig. 1*b*). Methylation levels of *RASSF1A* were significantly higher in the distal than in the proximal CRCs, as was also observed in the normal-appearing mucosae ($p < 0.05$, Fig. 1*b*). On the other hand, methylation levels of the four classical CIMP markers, *MLH1*, *MINT1*, *MINT2* *MINT31*, and a newly proposed CIMP marker, *RUNX3*[23], were significantly higher in the proximal than the distal CRCs. We also examined three genes, *MGMT*, *RASSF1A* and *SFRP1*, in 22 colon polyps (Fig. 1*b*). Several distal colon polyps showed higher methylation levels of *RASSF1A* and *MGMT* than proximal colon polyps, though the difference was not statistically significant.

These observations were also reproducible when CIMP-negative distal CRCs and CIMP-positive proximal CRCs were compared (Supporting Information Fig. 1). *RASSF1A* was most frequently methylated in distal CIMP-negative CRCs (51%, Fig. 1*c*). We also found that the methylation levels of *RASSF1A* were significantly higher in CIMP-negative than in CIMP-positive CRCs (mean, 18.3%; 95% CI, 14.6–22.0 *vs.* mean, 15.8%; 95% CI, 7.0–24.6; $p = 0.03$). In contrast, the five classical CIMP markers, as well as a new CIMP marker, *RUNX3*, were remarkably methylated in CIMP-positive CRCs. Five of six (83.3%) CRC cases with *BRAF* mutations fell into the proximal CIMP-positive group. Similarly, *RASSF1A* and *MGMT* were more frequently methylated in distal than in proximal colon polyps (Fig. 1*d*).

Concomitant methylation of *MGMT*, *RASSF1A* and *SFRP1* is correlated with age in distal normal-appearing mucosa from CRC cases

Substantial methylation of *MGMT*, *RASSF1A* and *SFRP1* was detected in normal-appearing mucosa from both CRC and colon polyp cases. We determined whether methylation of those three genes is associated with age and might occur concomitantly with methylation of the other loci. In distal normal-appearing mucosa from CRC cases, methylation levels of the three genes were significantly correlated with patient age (Pearson's correlation coefficients, *RASSF1A*, $r = 0.53$, $p < 0.01$; *SFRP1*, $r = 0.36$, $p < 0.01$; and *MGMT*, $r = 0.37$, $p < 0.01$), as well as with one another (all correlations with $p < 0.01$, Fig. 2*a*). In contrast, methylation levels of the genes in the proximal normal-appearing mucosa did not show strong correlations with patient age or with one another as was found in the distal colon (Fig. 2*a*).

In the normal-appearing mucosa from distal colon polyp cases, methylation levels of *RASSF1A* and *SFRP1* were significantly correlated with patient age (*RASSF1A*, $r = 0.42$, $p < 0.01$; and *SFRP1*, $r = 0.37$, $p = 0.03$; Fig. 2*b*), as was the case in CRC. No correlation was observed between the methylation levels of the three genes in the distal normal-appearing mucosae (Fig. 2*b*). Spearman's correlation coefficients calculated to evaluate the correlations yielded identical results (data not shown).

Interestingly, we found simultaneous methylation of the three target genes, *RASSF1A*, *SFRP1* and *MGMT*, affected the patient prognosis (Supporting Information Fig. 2). These data suggest that DNA methylation in multiple loci is simultaneously accumulated with aging in the distal normal-appearing mucosae in CRC cases and have the clinical impact for CRCs.

DNA methylation in normal-appearing mucosa as a clonal event

Densely methylated CpG promoters result in stable gene silencing.[24] To determine whether low or moderate overall levels of methylation in normal-appearing mucosae represent dense methylation in a subset of the cells in the sample or scattered methylation of different CpGs in a majority of the cells, we performed bisulfite sequences in *RASSF1A* and *MGMT* (Supporting Information Fig. 3). Several clones showed dense methylation in the *RASSF1A* and *MGMT* CpG promoter regions, implying that even in normal-appearing mucosa, a subset of cells harbors dense hypermethylation of tumor suppressor genes, which may be a component of a field defect.[13]

LINE-1 methylation status in CRCs and colon polyps

Aberrant global hypomethylation and regional promoter hypermethylation have been observed in many human malignancies[4]; however, it has not been well documented in non-cancerous tissues. To assess global DNA methylation in

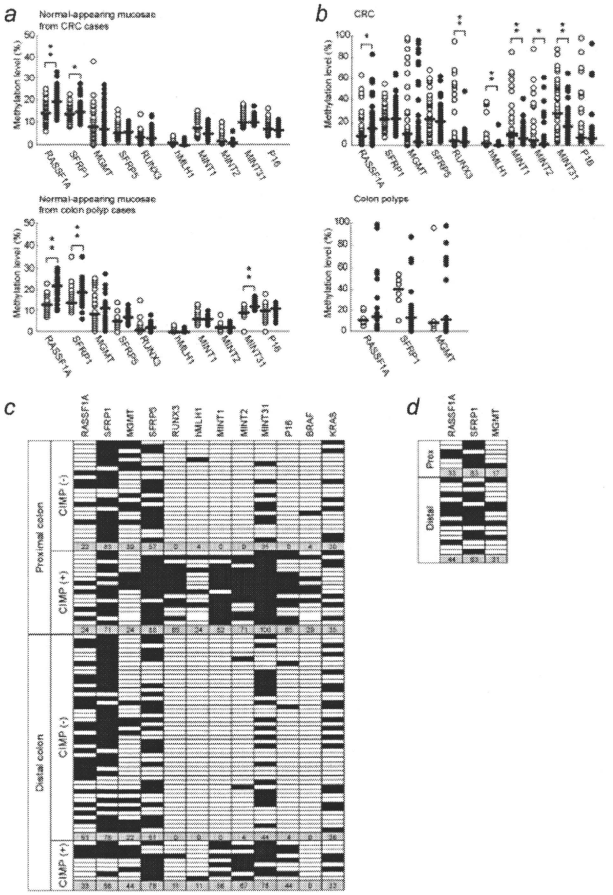

Figure 1. Distribution of the promoter methylation status of 10 genes (*RASSF1A*, *SFRP1*, *MGMT*, *SFRP5*, *RUNX3*, *hMLH1*, *MINT1*, *2* and *31* and *p16*). Levels of methylation measured by bisulfite pyrosequencing methylation analysis in CRC and colon polyp patients. Each circle represents the methylation level of normal-appearing mucosae from CRC or colon polyp cases (*a*) and cancerous tissues from CRC or colon polyp (*b*) from the proximal (white) or distal colon (black). Y-axis indicates the level of methylation of each gene. Horizontal bars denote median methylation levels for each group. *$p < 0.05$; **$p < 0.01$. Methylation frequencies and mutation status of CRC (*c*) and colon polyp patients (*d*). Each column represents the methylation status or *BRAF* or *KRAS* mutations in cancerous tissues or polyps. Black boxes denote methylation levels >15% (methylation positive) or mutations in the *KRAS* or *BRAF* genes. Numbers inside the gray boxes indicate the percentage of cases in which the gene was methylated or mutated. Samples with methylation of at least two of the five CIMP markers (*hMLH1*, *MINT1*, *2*, and *31* and *p16*) were considered CIMP positive. The proximal colon includes the cecum, ascending and transverse colon; the distal includes the descending and sigmoid colon, and the rectum.

Int. J. Cancer: **127**, 2095–2105 (2010) © 2010 UICC

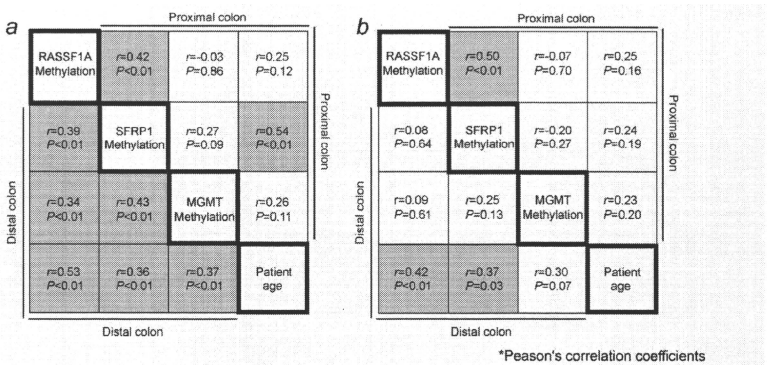

Figure 2. Correlation analysis between methylation levels of three genes (*MGMT*, *RASSF1A* and *SFRP1*) and patient age in the normal-appearing mucosae from CRC (*a*) and colon polyp patients (*b*). Upper right boxes indicate correlations for proximal colon samples, and lower left boxes indicate correlations for distal colon samples; *r* indicates Pearson's correlation coefficients. Colored boxes indicate a significant correlation ($p < 0.01$ or $p < 0.05$).

normal-appearing muocosa, *LINE-1* methylation, a good indicator of global methylation, was assessed by pyrosequencing (Fig. 3).[25,26] Significant hypomethylation was found in both CRCs and colon polyps compared with normal-appearing mucosae (Fig. 3*a*, $p < 0.01$). In CRCs, *LINE-1* methylation was significantly lower in the CIMP-negative than the CIMP-positive group (mean, 56.8%; 95% CI, 54.7–58.9 *vs.* mean, 60.9%; 95% CI, 56.9–65.0, $p < 0.05$). These are concordant with a previous large-scale study using the same technology.[26] Interestingly, correlation coefficient analysis revealed a clear inverse correlation between methylation levels and age in the distal normal-appearing mucosae ($r = -0.48$, $p < 0.01$; Fig. 3*b*). However, no such correlation was observed in the proximal normal-appearing mucosae of either CRC or colon polyp cases (Figs. 3*b* and 3*c*). Along with these findings, normal-appearing mucosae with two or more hypermethylated genes showed a significantly lower level of *LINE-1* methylation than mucosae with one or no hypermethylated genes (mean, 67.0%; 95% CI, 65.4–68.6 *vs.* mean, 69.1%; 95% CI, 67.7–70.3, $p < 0.05$, Fig. 3*d*). These data suggest that in a subset of distal CRC cases, the normal-appearing mucosa becomes susceptible to age-related methylation, wherein even global DNA methylation is affected, and regional hypermethylation and global hypomethylation occur simultaneously in the same individuals.

Genome-wide methylation analysis of CIMP-negative and CIMP-positive CRCs

To decipher the global DNA methylation targets of CIMP-negative cancers, especially of distal CRCs, we performed MCAM in 18 CRCs: 7 CIMP-positive proximal CRCs and 11 CIMP-negative distal CRCs (Materials and methods, and Supporting Information Table 2). We previously reported that a signal ratio of Cy5/Cy3 in excess of 2.0 in MCAM is concordant with hypermethylation status in pyrosequencing analysis.[16] In this study, we validated the MCAM data (Cy5/Cy3>2.0 as methylation positive) with pyrosequencing assays and found that the specificity and sensitivity were both 77% (Supporting Information Table 4). Unsupervised hierarchical clustering analysis using 6,157 genes showed that CIMP-positive proximal CRCs had a prominent cluster of hypermethylated genes, confirming the five classical CIMP markers as reliable predictive markers for CIMP (Fig. 4*a*). Consistently, larger numbers of hypermethylated genes were observed in CIMP-positive proximal CRCs than in CIMP-negative distal CRCs (average of 1,321 genes *vs.* 1,112 genes, $p < 0.05$, Fig. 4*b*).

Although CIMP-positive proximal CRCs were classified by the five classical CIMP markers, four new CIMP markers, *RUNX3*, *CACNA1G*, *NEUROG1* and *CRABP1*, were also highly positive in these CRCs (Fig. 4*c*).[23,27] However, another two new CIMP markers, *SOCS1* and *IGF2*, were not more predictive than the five classical CIMP markers. We noted that mutations in the *BRAF* gene were found in CIMP-positive proximal CRCs, whereas mutations in the *p53* gene appeared in CIMP-negative distal CRCs.

Among the 1,224 genes identified from MCAM data that were methylated in more than half the CRC cases (*i.e.*, in more than 4/7 of the CIMP-positive proximal CRCs and 6/11 of the CIMP-negative distal CRCs), more genes were

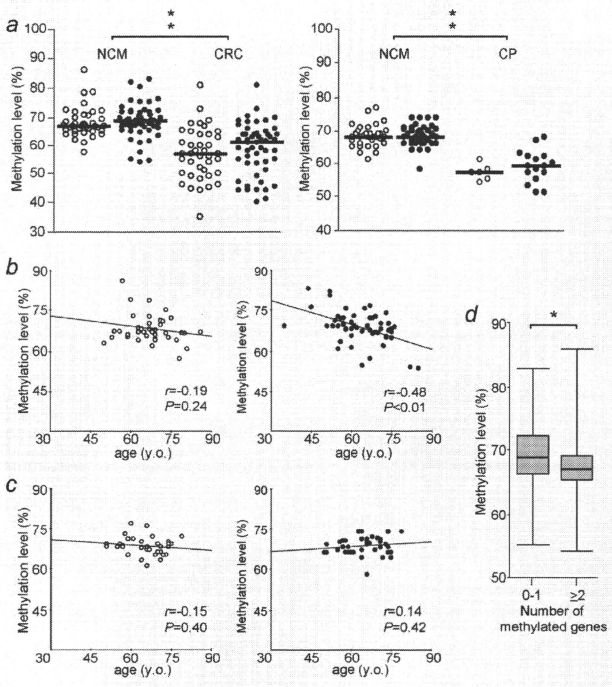

Figure 3. Distribution of *LINE-1* promoter methylation levels measured by bisulfite pyrosequencing methylation analysis in CRC and colon polyp patients. (*a*) Each circle represents the methylation level of normal-appearing mucosa, CRC and colon polyp from the proximal (white) and distal colon (black). Horizontal lines represent median methylation levels for each group. Scatter plots of *LINE-1* methylation level *vs.* patient age in normal-appearing mucosa from CRC (*b*) and colon polyp patients (*c*) taken from the proximal (white circles) or distal colon (black circles). (*d*) Box-and-whisker plot of *LINE-1* methylation level in normal-appearing mucosae with hypermethylation detected in 0–1 or ≥2 of 3 genes, *RASSF1A*, *SFRP1* and *MGMT*. The mean is marked by a bold line inside the box whose ends denote the upper and lower quartiles. Error bars represent 5 and 95 percentile values. $*p < 0.05$; $**p < 0.01$.

methylated in CIMP-positive proximal CRC than CIMP-negative distal CRCs (1,056 genes *vs.* 504 genes, among which 336 genes were commonly methylated in both groups, $p < 0.01$, Fig. 5*a*). This tendency was also true when analyzing genes methylated in at least 30% of CRC cases ($p < 0.01$). Although CIMP-positive proximal CRCs appear to be more robustly affected by DNA methylation, there is a subset of genes preferentially methylated in CIMP-negative distal CRCs.

Combined array data analysis of CRCs and eight normal-appearing mucosae revealed that DNA methylation in either both normal-appearing mucosae and CRCs (age-related methylation, type A genes), or specifically in CRCs (cancer-specific methylation, type C genes).[5] The ratios of type A to type C genes in CIMP-negative distal CRCs and CIMP-positive proximal CRCs were significantly different. More than half of the hypermethylated genes in CIMP-negative distal CRCs were also methylated in the normal-appearing mucosae, as opposed to CIMP-positive proximal CRCs, where more than 60% of hypermethylated genes were cancer specific ($p < 0.01$, Fig. 5*b*). A heat-map overview of 168 genes (type C, 79 genes; type A, 89 genes), which were methylated in more than half of CIMP-negative distal CRCs revealed that DNA methylation was also found in CIMP-positive

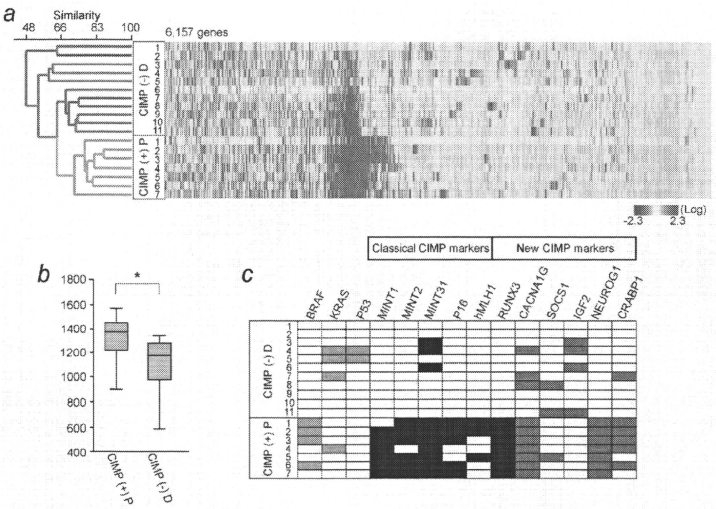

Figure 4. MCAM analysis of CRC cases. (*a*) Heat-map overview and cluster analysis of hierarchical cluster analysis using the DNA methylation status of 18 samples [11 CIMP-negative distal CRCs (CIMP (−) D), and 7 CIMP-positive proximal CRCs (CIMP (+) P)]. Red, yellow and blue in the cells reflect methylation levels as indicated in the scale bar below the matrix (log2-transformed scale). All 7 CIMP-positive CRCs fall into one subgroup (blue line). (*b*) Box-and-whisker plot showing the number of methylated genes in CIMP-positive proximal CRCs and CIMP-negative distal CRCs. The median is marked by a bold line inside the box whose ends represent the upper and lower quartiles. Error bars denote 5 and 95 percentile values. $*p < 0.05$. (*c*) Comparison of methylation status of CIMP-positive and CIMP-negative CRCs. Each column represents the mutation or methylation status of each CRC case. Blue boxes indicate mutations in the *KRAS*, *BRAF* or *p53* genes. Black and red boxes indicate a methylation-positive status determined by pyrosequencing or MCAM analysis (average Cy3/Cy5 signal ratio > 2.0), respectively.

proximal CRCs in a certain extend (Fig. 5*c*). We further validated the identified hypermethylated genes in CIMP-negative distal CRCs. Methylation levels of *HOXA5* (type A gene) and *PDE10A* (type C gene) were examined by pyrosequencing in CRCs and their corresponding normal-appearing mucosae (Fig. 5*d*). In the normal-appearing mucosae of CRC cases, DNA methylation levels of both genes were significantly higher in the distal than the proximal colon (HOXA5, $p < 0.05$; PDE10A, $p < 0.01$). DNA methylation levels of *PDE10A* genes were also higher in the distal than the proximal CRCs ($p < 0.01$).

Discussion

Alterations in DNA methylation represent epigenetic phenomena that appear to be early events in tumorigenesis.[28] Recent comprehensive studies have suggested that CIMP is a distinct colon tumorigenesis pathway that shows an accumulation of high rates of aberrant promoter methylation events. CIMP tumors have a characteristic phenotype with such features as *BRAF* or *KRAS* mutations, a specific histology (mucinous or poorly differentiated) and proximal location.[3,6,27,29–31] In addition, cancer-specific DNA methylation is more frequent than age-related DNA methylation in a subclass of CIMP-positive CRCs.[6] The CIMP-positive tumors we analyzed exhibited these features; however, we also found frequent methylation of some genes in the CIMP-negative distal CRCs. This suggests that during colon tumorigenesis, other mechanisms besides CIMP could be causing aberrant DNA methylation in the distal colon.

By focusing on the differences in hypermethylated genes between CIMP-positive proximal and CIMP-negative distal CRCs, our genome-wide analysis revealed that hypermethylated genes in the CIMP-negative distal CRCs largely overlapped with those in the CIMP-positive proximal CRCs; however, a set of genes was preferentially methylated in the CIMP-negative distal CRCs. Along with *RASSF1A* and *SFRP1*, two identified genes, *HOXA5* and *PDE10A*, were also frequently methylated in distal normal-appearing mucosae

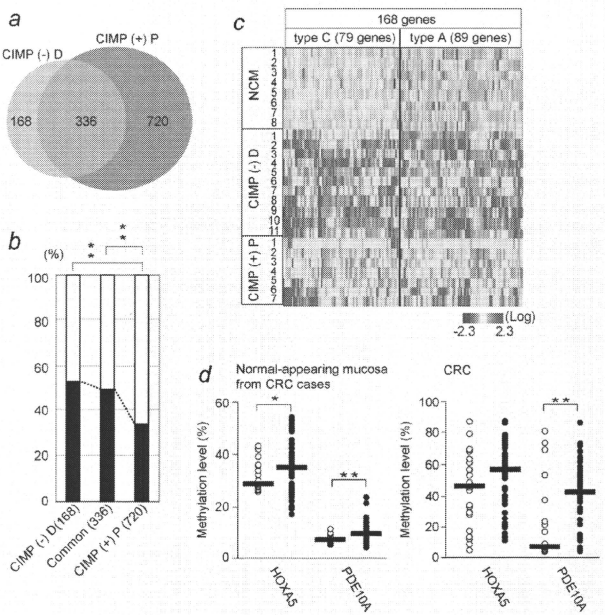

Figure 5. MCAM and pyrosequencing analysis associated with CIMP-negative distal CRCs. (*a*) Venn diagram illustrating the number of genes that were methylation positive in more than half of CRC cases as determined by MCAM. More genes were methylated in CIMP-positive proximal CRCs than CIMP-negative distal CRCs (1,056 genes *vs.* 504 genes, among which 336 genes were commonly methylated in both groups). (*b*) Percentages of type A (black box) and type C (white box) genes among CIMP-negative distal (CIMP (–) D), CIMP-positive proximal (CIMP (+) P) CRCs and both (common). $^{**}p < 0.01$. (*c*) Heat-map overview with 168 genes which were methylation positive in more than half of CIMP-negative distal CRC cases. Red, yellow and blue in the cells reflect methylation levels as indicated in the scale bar below the matrix (log2-transformed scale). (*d*) Levels of methylation in *HOXA5* and *PDE10A* measured by bisulfite pyrosequencing methylation analysis in CRC cases. Each circle represents the methylation levels of normal-appearing mucosae (*b*) and CRCs (*c*) from the proximal (white) or distal colon (black). $^{*}p < 0.05$; $^{**}p < 0.01$.

and CRCs. HOXA5, a developmental regulator of several tissues, has also been known to act as a tumor suppressor through induction of apoptosis of cancer cells.[32–34] A homozygous deletion at 6q26-27, which includes the *PDE10A* genes, has been observed in glioblastoma.[35] Simultaneous silencing of these sets of genes by epigenetic mechanisms in addition to genetic alteration (*e.g.*, mutations in the *p53* gene) may contribute the distal colon tumorigenesis.

The multistep carcinogenesis of CRCs has suggested the existence of a period of preneoplastic condition, field defect, in which cells accumulate genetic and epigenetic alterations and are predisposed to tumor development.[2,36,37] Age-related epigenetic defects have been proposed as potential sources of the field defect in colon carcinogenesis.[13,38] In this study, we analyzed the DNA methylation status of normal-appearing mucosae to elicit the DNA methylation behavior of distal CRC compared with proximal CRC. In the distal normal-appearing mucosae of CRCs, methylation levels of *RASSF1A*, *SFRP1* and *MGMT* were significantly correlated with one another and associated with age, whereas global methylation levels (estimated as *LINE-1* methylation levels) diminished with age. Both regional hypermethylation and global hypomethylation appear to occur simultaneously in a subset of distal normal-appearing mucosae. These data indicated that distal CRCs might be closely associated by field defect where age-related DNA methylation target genes were embedded,

involving the pathways and providing the cell with selective advantages that promote tumor progression.

The characteristic DNA methylation behavior in distal normal-appearing mucosa and CRCs may be partially explained by various environmental factors in the distal colon, where continuous exposure to stool is common.[9,10,39–42] In addition, absorption of water from the stool increases the risk of exposure to higher concentrations of exogenous substances that may act as epimutagenes, proposed environmental factors that can affect the epigenetic status of genes.[30,42] The levels of exposure to environmental factors, patterns of genetic defects and types of epimutagenes present differ in each case by location and may affect epigenetic variations. Consequently, accumulation patterns of DNA methylation in normal-appearing mucosae is not uniform by location, as the present study also indicates.

Although the fundamental cause of aberrant DNA methylation in cancers is still under investigation, combinations of such environmental exposures and genetic alterations might facilitate the deregulation of epigenetic control. In cancer cell lines, hypermethylation is triggered by low and random levels of DNA methylation (seeding) together with gene inactivation by the removal of Sp1 transcription factor binding sites.[43] An Sp1/Sp3 binding polymorphism in the *RIL* promoter has also been reported to confer methylation protection.[44] Dysregulation of such *cis*-acting factors in addition to environmental exposures may be pivotal in perpetuating the hypermethylation of a subset of genes. Nevertheless, our study showed here that different mechanisms of acquiring epigenetic changes may be present during the tumorigenesis of CRCs.

In conclusion, our comprehensive analysis deciphered that particular patterns of aberrant DNA methylation in CIMP-negative distal CRCs are active during colon tumorigenesis; global DNA methylation levels were decreased and age-related DNA methylation in multiple genes was inappropriately induced, which may dictate a characteristic pathogenesis. Because recent combined genetic and epigenetic analyses of sporadic CRC suggest that there are different subsets possessing distinct clinicopathological features,[45] elucidation of the precise roles of epigenetic abnormalities might be a great help for the prevention, screening and treatment of CRCs.

Acknowledgements

We wish to thank Ms. Ikuko Tomimatsu for her technical assistance and Ms. Shana Straub for her advice and critical reading of the manuscript.

References

1. Vogelstein B, Kinzler KW. Cancer genes and the pathways they control. *Nat Med* 2004;10:789–99.
2. Kinzler KW, Vogelstein B. Lessons from hereditary colorectal cancer. *Cell* 1996;87: 159–70.
3. Issa JP. CpG island methylator phenotype in cancer. *Nat Rev Cancer* 2004;4:988–93.
4. Jones PA, Baylin SB. The fundamental role of epigenetic events in cancer. *Nat Rev Genet* 2002;3:415–28.
5. Toyota M, Ahuja N, Ohe-Toyota M, Herman JG, Baylin SB, Issa JP. CpG island methylator phenotype in colorectal cancer. *Proc Natl Acad Sci U S A* 1999;96:8681–6.
6. Shen L, Toyota M, Kondo Y, Lin E, Zhang L, Guo Y, Hernandez NS, Chen X, Ahmed S, Konishi K, Hamilton SR, Issa JP. Integrated genetic and epigenetic analysis identifies three different subclasses of colon cancer. *Proc Natl Acad Sci U S A* 2007;104: 18654–9.
7. Issa JP Optimizing therapy with methylation inhibitors in myelodysplastic syndromes: dose, duration, and patient selection. *Nat Clin Pract Oncol* 2005;2: S24–9.
8. Baylin SB, Ohm JE. Epigenetic gene silencing in cancer—a mechanism for early oncogenic pathway addiction? *Nat Rev Cancer* 2006;6:107–16.
9. Bufill JA. Colorectal cancer: evidence for distinct genetic categories based on proximal or distal tumor location. *Ann Intern Med* 1990;113:779–88.
10. Breivik J, Lothe RA, Meling GI, Rognum TO, Borresen-Dale AL, Gaudernack G. Different genetic pathways to proximal and distal colorectal cancer influenced by sex-related factors. *Int J Cancer* 1997;74: 664–9.
11. Deng G, Kakar S, Tanaka H, Matsuzaki K, Miura S, Sleisenger MH, Kim YS. Proximal and distal colorectal cancers show distinct gene-specific methylation profiles and clinical and molecular characteristics. *Eur J Cancer* 2008;44:1290–301.
12. Azzoni C, Bottarelli L, Campanini N, Di Cola G, Bader G, Mazzeo A, Salvemini C, Morari S, Di Mauro D, Donadei E, Roncoroni L, Bordi C, et al. Distinct molecular patterns based on proximal and distal sporadic colorectal cancer: arguments for different mechanisms in the tumorigenesis. *Int J Colorect Dis* 2007;22: 115–26.
13. Shen L, Kondo Y, Rosner GL, Xiao L, Hernandez NS, Vilaythong J, Houlihan PS, Krouse RS, Prasad AR, Einspahr JG, Buckmeier J, Alberts DS, et al. MGMT promoter methylation and field defect in sporadic colorectal cancer. *J Natl Cancer Inst* 2005;97:1330–8.
14. Clark SJ, Harrison J, Paul CL, Frommer M. High sensitivity mapping of methylated cytosines. *Nucleic Acids Res* 1994;22: 2990–7.
15. Colella S, Shen L, Baggerly KA, Issa JP, Krahe R. Sensitive and quantitative universal Pyrosequencing methylation analysis of CpG sites. *Biotechniques* 2003; 35:146–50.
16. Gao W, Kondo Y, Shen L, Shimizu Y, Sano T, Yamao K, Natsume A, Goto Y, Ito M, Murakami H, Osada H, Zhang J, et al. Variable DNA methylation patterns associated with progression of disease in hepatocellular carcinomas. *Carcinogenesis* 2008;29:1901–10.
17. Toyota M, Ahuja N, Suzuki H, Itoh F, Ohe-Toyota M, Imai K, Baylin SB, Issa JP. Aberrant methylation in gastric cancer associated with the CpG island methylator phenotype. *Cancer Res* 1999;59:5438–42.
18. Shen L, Kondo Y, Guo Y, Zhang J, Zhang L, Ahmed S, Shu J, Chen X, Waterland RA, Issa JP. Genome-wide profiling of DNA methylation reveals a class of normally methylated CpG island promoters. *PLoS Genet* 2007;3:2023–36.
19. Eisen MB, Spellman PT, Brown PO, Botstein D. Cluster analysis and display of genome-wide expression patterns. *Proc Natl Acad Sci U S A* 1998;95:14863–8.
20. Spittle C, Ward MR, Nathanson KL, Gimotty PA, Rappaport E, Brose MS, Medina A, Letrero R, Herlyn M, Edwards RH. Application of a BRAF pyrosequencing assay for mutation detection and copy number analysis in malignant melanoma. *J Mol Diagn* 2007;9: 464–71.
21. Ogino S, Meyerhardt JA, Cantor M, Brahmandam M, Clark JW, Namgyal C, Kawasaki T, Kinsella K, Michelini AL,

Enzinger PC, Kulke MH, Ryan DP, et al. Molecular alterations in tumors and response to combination chemotherapy with gefitinib for advanced colorectal cancer. *Clin Cancer Res* 2005;11:6650–6.
22. Goto Y, Shinjo K, Kondo Y, Shen L, Toyota M, Suzuki H, Gao W, An B, Fujii M, Murakami H, Osada H, Taniguchi T, et al. Epigenetic profiles distinguish malignant pleural mesothelioma from lung adenocarcinoma. *Cancer Res* 2009;69: 9073–82.
23. Weisenberger DJ, Siegmund KD, Campan M, Young J, Long TI, Faasse MA, Kang GH, Widschwendter M, Weener D, Buchanan D, Koh H, Simms L, et al. CpG island methylator phenotype underlies sporadic microsatellite instability and is tightly associated with BRAF mutation in colorectal cancer. *Nat Genet* 2006;38: 787–93.
24. Kass SU, Landsberger N, Wolffe AP. DNA methylation directs a time-dependent repression of transcription initiation. *Curr Biol* 1997;7:157–65.
25. Yang AS, Estecio MR, Doshi K, Kondo Y, Tajara EH, Issa JP A simple method for estimating global DNA methylation using bisulfite PCR of repetitive DNA elements. *Nucleic Acids Res* 2004;32:e38.
26. Ogino S, Kawasaki T, Nosho K, Ohnishi M, Suemoto Y, Kirkner GJ, Fuchs CS. LINE-1 hypomethylation is inversely associated with microsatellite instability and CpG island methylator phenotype in colorectal cancer. *Int J Cancer* 2008;122: 2767–73.
27. Ogino S, Cantor M, Kawasaki T, Brahmandam M, Kirkner GJ, Weisenberger DJ, Campan M, Laird PW, Loda M, Fuchs CS. CpG island methylator phenotype (CIMP) of colorectal cancer is best characterised by quantitative DNA methylation analysis and prospective cohort studies. *Gut* 2006;55:1000–6.
28. Jones PA, Laird PW. Cancer epigenetics comes of age. *Nat Genet* 1999;21:163–7.
29. Issa JP, Shen L, Toyota M. CIMP, at last. *Gastroenterology* 2005;129:1121–4.
30. Grady WM. CIMP and colon cancer gets more complicated. *Gut* 2007;56: 1498–500.
31. Nagasaka T, Koi M, Kloor M, Gebert J, Vilkin A, Nishida N, Shin SK, Sasamoto H, Tanaka N, Matsubara N, Boland CR, Goel A. Mutations in both KRAS and BRAF may contribute to the methylator phenotype in colon cancer. *Gastroenterology* 2008;134:1950–60.
32. Raman V, Martensen SA, Reisman D, Evron E, Odenwald WF, Jaffee E, Marks J, Sukumar S. Compromised HOXA5 function can limit p53 expression in human breast tumours. *Nature* 2000;405: 974–8.
33. Shiraishi M, Sekiguchi A, Terry MJ, Oates AJ, Miyamoto Y, Chuu YH, Munakata M, Sekiya T. A comprehensive catalog of CpG islands methylated in human lung adenocarcinomas for the identification of tumor suppressor genes. *Oncogene* 2002;21: 3804–13.
34. Chen H, Zhang H, Lee J, Liang X, Wu X, Zhu T, Lo PK, Zhang X, Sukumar S. HOXA5 acts directly downstream of retinoic acid receptor beta and contributes to retinoic acid-induced apoptosis and growth inhibition. *Cancer Res* 2007;67: 8007–13.
35. Yin D, Ogawa S, Kawamata N, Tunici P, Finocchiaro G, Eoli M, Ruckert C, Huynh T, Liu G, Kato M, Sanada M, Jauch A, et al. High-resolution genomic copy number profiling of glioblastoma multiforme by single nucleotide polymorphism DNA microarray. *Mol Cancer Res* 2009;7:665–77.
36. Slaughter DP, Southwick HW, Smejkal W. Field cancerization in oral stratified squamous epithelium; clinical implications of multicentric origin. *Cancer* 1953;6: 963–8.
37. Ushijima T. Epigenetic field for cancerization. *J Biochem Mol Biol* 2007;40: 142–50.
38. Issa JP, Ottaviano YL, Celano P, Hamilton SR, Davidson NE, Baylin SB. Methylation of the oestrogen receptor CpG island links ageing and neoplasia in human colon. *Nat Genet* 1994;7:536–40.
39. Wynder EL, Reddy BS, Weisburger JH. Environmental dietary factors in colorectal cancer. Some unresolved issues. *Cancer* 1992;70:1222–8.
40. Elsaleh H, Joseph D, Grieu F, Zeps N, Spry N, Iacopetta B. Association of tumour site and sex with survival benefit from adjuvant chemotherapy in colorectal cancer. *Lancet* 2000;355:1745–50.
41. Iacopetta B. Are there two sides to colorectal cancer? *Int J Cancer* 2002;101: 403–8.
42. Guarner F, Malagelada JR. Gut flora in health and disease. *Lancet* 2003;361:512–9.
43. Song JZ, Stirzaker C, Harrison J, Melki JR, Clark SJ. Hypermethylation trigger of the glutathione-S-transferase gene (GSTP1) in prostate cancer cells. *Oncogene* 2002;21: 1048–61.
44. Boumber YA, Kondo Y, Chen X, Shen L, Guo Y, Tellez C, Estecio MR, Ahmed S, Issa JP. An Sp1/Sp3 binding polymorphism confers methylation protection. *PLoS Genet* 2008;4:e1000162.
45. Issa JP. Colon cancer: it's CIN or CIMP. *Clin Cancer Res* 2008;14:5939–40.

Cancer Chemother Pharmacol (2010) 66:237–243
DOI 10.1007/s00280-009-1151-1

ORIGINAL ARTICLE

Relationship of mRNA expressions of RanBP2 and topoisomerase II isoforms to cytotoxicity of amrubicin in human lung cancer cell lines

Yoshitsugu Horio · Hirotaka Osada · Junichi Shimizu · Shizu Ogawa · Toyoaki Hida · Yoshitaka Sekido

Received: 3 March 2009 / Accepted: 22 September 2009 / Published online: 7 October 2009

Abstract
Purpose RanBP2 is a small ubiquitin-like modifier ligase for DNA topoisomerase II (TopoII) and plays a role in maintaining chromosome stability by recruiting TopoII to centromeres during mitosis. Engineered-mice with low amounts of RanBP2 have been reported to form lung adenocarcinomas. Furthermore, in the murine embryonic fibroblasts, formation of chromatin bridges in anaphase, a distinctive feature of cells with impaired DNA decatenation by chemical inhibition of TopoII, has been reported. In this study, we tested whether the association between mRNA expression of the RanBP2 gene and chemosensitivity of a TopoII inhibitor, amrubicin could be seen.
Methods Using a panel of 20 lung cancer cell lines, the mRNA expression levels of the RanBP2, TopoII-alpha and TopoII-beta genes were examined by quantitative real-time reverse transcription PCR. The in vitro cytotoxicity of amrubicin was assessed using a tetrazolium-based colorimetric assay (MTT assay).
Results Although RanBP2 mRNA expression was infrequently downregulated in human lung cancer cell lines, significantly higher RanBP2 transcripts were observed in small cell lung cancer than non-small cell lung cancer. There were no correlations between chemosensitivity of amrubicin and mRNA expression levels of the RanBP2, TopoII-alpha and TopoII-beta genes.
Conclusions Our in vitro results suggest that mRNA expressions of RanBP2 and TopoII isoforms are unlikely to be a predictive biomarker for the sensitivity to amrubicin.

Keywords SUMO ligase · Topoisomerase II inhibitor · Predictive biomarker · Chromosomal instability · Lung cancer

Y. Horio (✉) · J. Shimizu · S. Ogawa · T. Hida
Department of Thoracic Oncology, Aichi Cancer Center Hospital, 1-1 Kanokoden, Chikusa-ku, Nagoya 464-8681, Japan
e-mail: yhorio@aichi-cc.jp

H. Osada · Y. Sekido
Division of Molecular Oncology, Aichi Cancer Center Research Institute, 1-1 Kanokoden, Chikusa-ku, Nagoya 464-8681, Japan

Introduction

Lung cancer is a leading cause of cancer mortality in the United States and in Japan [13, 29]. Lung cancer has two main types: small cell lung cancer (SCLC) and non-SCLC (NSCLC). The major histological subtypes of NSCLC include adenocarcinoma, squamous carcinoma and large cell carcinoma. About 15% of lung cancers are SCLC. SCLC spreads rapidly and widely forming additional large tumors in lymph nodes, bones, adrenal glands, liver and brain. Because of its aggressive nature the overall survival of SCLC is worse than that of NSCLC and only 5–10% at 5 years. Survival of patients with either SCLC or NSCLC is strongly correlated with the stage of disease. For patients with advanced tumors, the prognosis is dismal because the available treatment regimens such as chemotherapy and radiation therapy are essentially palliative and primarily serve only to prolong survival. In fact, combination chemotherapy with etoposide plus cisplatin or irinotecan plus cisplatin for extensive-stage (ES) SCLC as well as the common first-line platinum-based combination regimens for advanced NSCLC only produced a median survival time of about 1 year [18, 19, 23]. Thus, new treatment approaches are clearly required.

Amrubicin, developed and approved in Japan for the treatment of SCLC and NSCLC, is a totally synthetic